

PROJECT ID: BAT461

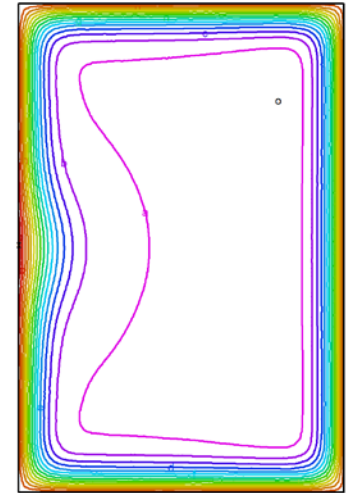
QUANTIFYING HETEROGENEITIES/ DEGRADATION DURING FAST CHARGE

ANDREW COLCLASURE
National Renewable Energy Laboratory
(NREL)



eXtreme Fast Charge Cell Evaluation
of Lithium-ion Batteries

**Saturation
Distribution**



This presentation does not contain any proprietary, confidential, or otherwise restricted information

DOE Vehicle Technologies Program
2020 Annual Merit Review
and Peer Evaluation Meeting
June 1–4, 2020

OVERVIEW

Timeline

- Start: October 1, 2017
- End: September 30, 2021
- Percent Complete: 75%

Budget

- Funding for FY20 – \$5.6M

Barriers

- Cell degradation during fast charge
- Low energy density and high cost of fast charge cells

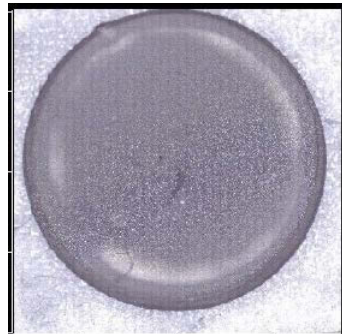
Partners

- Argonne National Laboratory
- Idaho National Laboratory
- Lawrence Berkeley National Lab
- National Renewable Energy Laboratory
- SLAC National Accelerator Lab
- Oak Ridge National Lab

RELEVANCE

- Lithium plating and cell degradation during fast charge are often driven by local heterogeneities across length scales ranging from cm to microns
- Goal: Detect/quantify how and what local heterogeneities lead to early onset of lithium plating and cell degradation
 - Investigate cause of observed visual plating patterns
 - Determine if local variations in state of charge (SOC)/lithium plating are driven by local changes in microstructure properties
 - Develop a better fundamental understanding of lithium intercalation/staging, diffusion, and plating process.

Lithium Ring on Coin Cell
Electrode



Cell-scale heterogeneities

*Ira Bloom
(ANL)*



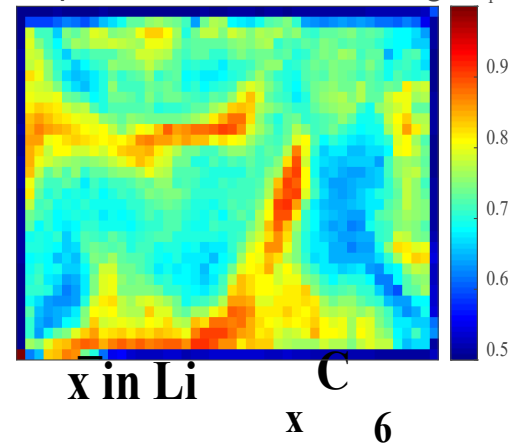
FY2020 MILESTONES

Milestone	Due	Status
Determine framework for kinetic model to more accurately predict lithium plating and determine parameters needed	3/31/2020	Completed
Publish results for kinetics lithium-plating model	9/30/2020	On-track
Quantify effect of edge/basal plane on intercalation/lithium kinetics	9/30/2020	On-track
Mapping of electrode microstructure heterogeneities overlaid with SOC, intercalated lithium, and lithium plating	9/30/2020	On-track

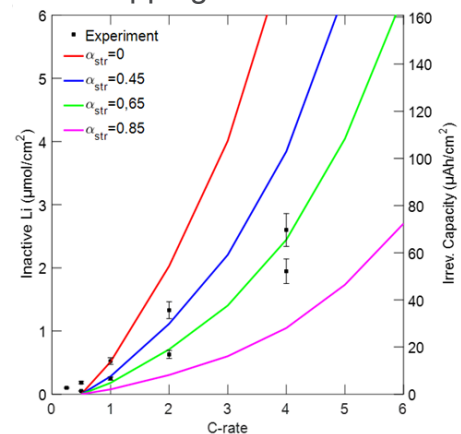
APPROACH

- Multi-lab and university team is investigating heterogeneity at several length scales through both experimentation and computational modeling.
- Specific activities include
 - Mapping of local SOC, cyclable lithium, and plated lithium using high-energy X-ray diffraction (XRD)
 - Mapping of local electrode microstructure properties
 - Modeling of electrolyte wetting process
 - Development of kinetic lithium-plating model
 - Quantification of intercalation and plating process on Edge vs. Basal plane sites
 - Kinetic Monte Carlo modeling of lithium intercalation process
 - Electrochemical microstructure modeling
 - Effect of pressure on extreme fast-charging (XFC) performance/degradation.

Intercalation fraction map for graphite anode in pouch cell after 6C charge



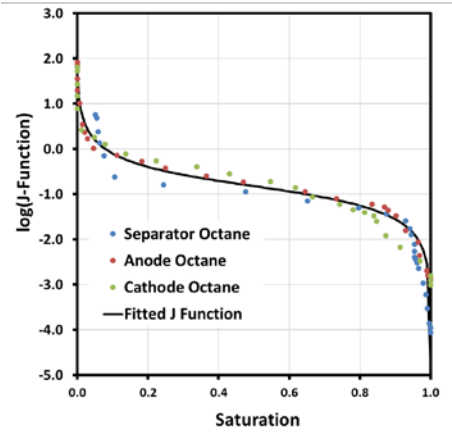
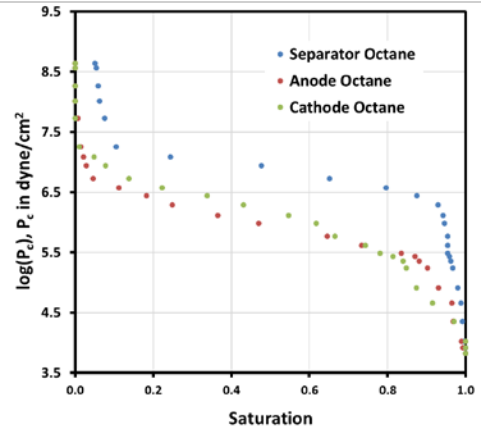
Dead lithium measured via gas titration compared with initial lithium plating model using different stripping efficiencies



WETTING MODEL AND PARAMETER DEVELOPMENT

- Standard two-phase flow model adapted for cell-wetting studies.
- Parameters provided by Kevin Gering's Advanced Electrolyte Model (AEM) and Standard Contact Porosimetry studies on cell components.

Standard Contact Porosimetry Studies



- Driving force for wetting is high. Capillary pressure above a psi till approximately 90% saturation (1 atmosphere = ~10⁶ dyne/cm²)
- Relative permeability of gas (κ_g) near full saturation most uncertain parameter
- J-function significantly reduces the layer variation for capillary pressure expression.

Darcy Flow

$$v_g = K \frac{\kappa_g}{\mu_g} (\nabla P_g - \rho_g \vec{g})$$

$$v_l = K \frac{\kappa_l}{\mu_l} (\nabla P_l - \rho_l \vec{g})$$

Mass Balances

$$\frac{\partial (\rho_g \epsilon (s - 1))}{\partial t} = -\nabla \cdot (\rho_g v_g)$$

$$\frac{\partial (\rho_l \epsilon s)}{\partial t} = -\nabla \cdot (\rho_l v_l)$$

J-Function Equation

$$P_c = \gamma \left(\frac{\epsilon}{K} \right)^{1/2} J(s)$$

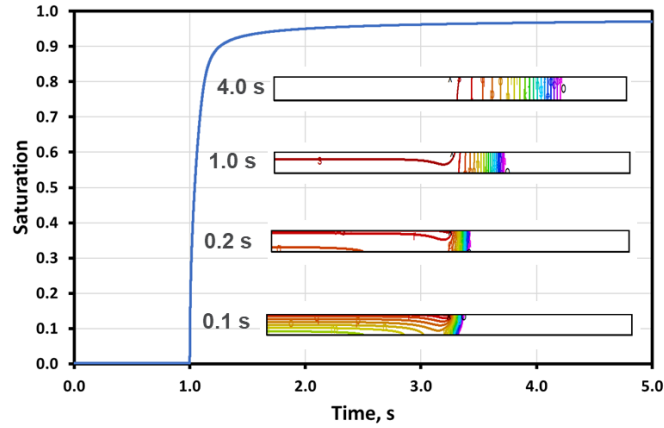
Pressure Relation

$$P_c = P_g - P_l$$

TWO-STEP PROCESS FOR WETTING OF A POUCH CELL

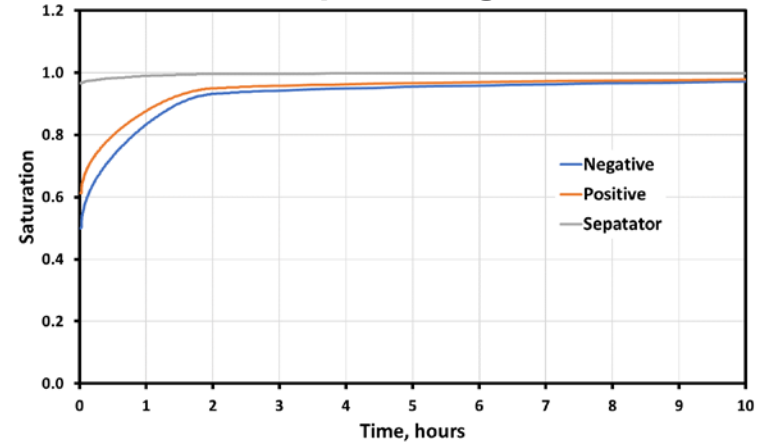
- When electrolyte is first added to the cell, it is physically worked around the cell and between the layers
- After the electrolyte is added and the cell is sealed, it is placed horizontally under a few psi of pressure and the remaining saturation occurs from the edges.

First Step: Negative Electrode Saturation



- During first step, electrodes are quickly saturated from their face
- Any electrolyte worked between layers is rapidly absorbed.

Second Step: Average Saturation



- The process for electrolyte seeping in through the edges is much slower than traveling across layers
- Electrolyte tends to build up at all edges, eventually trapping some gas, which can slowly be removed if there is a path.

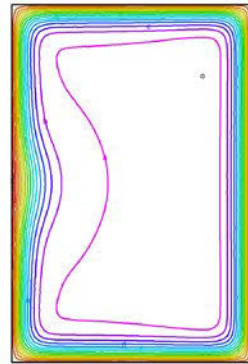
- One millimeter of wetted surface area and one millimeter of dry surface area
- Saturation distribution (red > orange > yellow > green > blue > indigo > violet).

CONNECTING SATURATION WITH LI PLATING

A two-dimensional electrochemical model was developed for Round 2 cells, with NREL-estimated tortuosities, to examine the impact of nonuniform wetting. Cell saturation distributions were obtained from simulations.

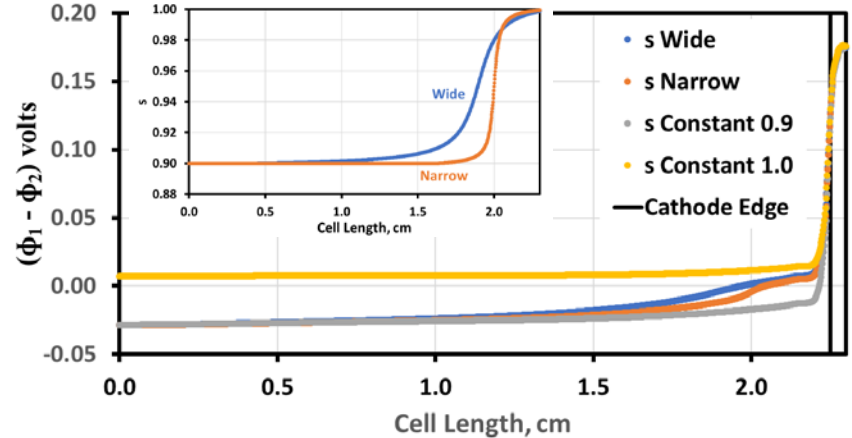


Saturation Distribution



1.0 (red >
orange >
yellow >
green >
blue >
indigo >
violet) 0.9

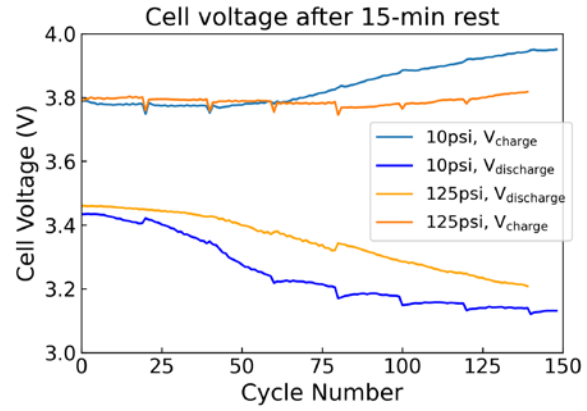
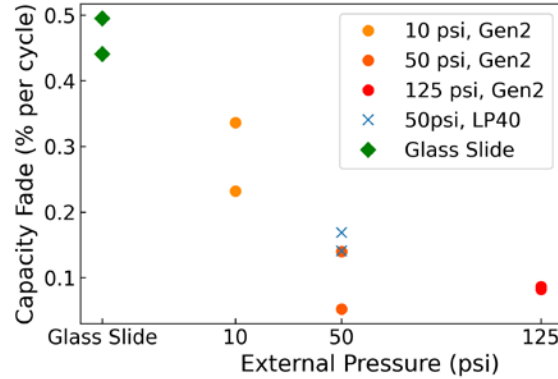
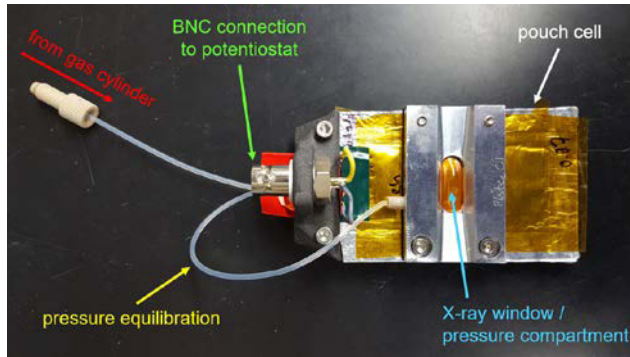
Negative Electrode Overpotential Next to Separator
2m Into a 6C Charge



- In the graph, lithium plating is possible at negative potentials and the lower the potential the more likely lithium plating will occur.
- The sharp rise in potential at the cathode edge is associated with the extended negative electrode. The more gradual rise further in is associated with the nonuniform saturation.
- As the charge proceeds, the potential curves are shifted more negative.

PRESSURE DEPENDENCE IN XFC BATTERIES

In-house designed air-pressure cell: precise control of pressure



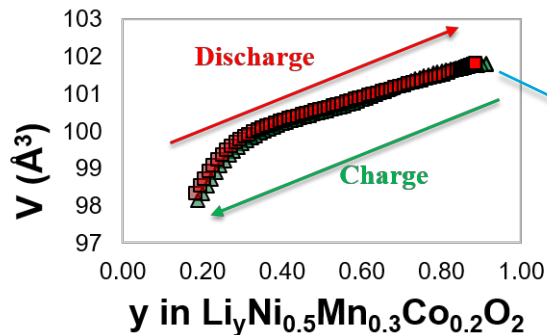
- External Pressure \uparrow , XFC capacity \uparrow for 70-micron electrodes (Round 2)
- External pressure \uparrow , capacity fade \downarrow
 - Pressure \uparrow , the depth of charge/discharge of active material \downarrow
 - At lower pressure, more active material becomes inactive
- Need to quantify pressure distribution in standard setups.

QUANTIFYING LATTICE-LITHIUM HETEROGENEITY IN CATHODE AND ANODE VIA *IN SITU* MAPPING

Operating conditions

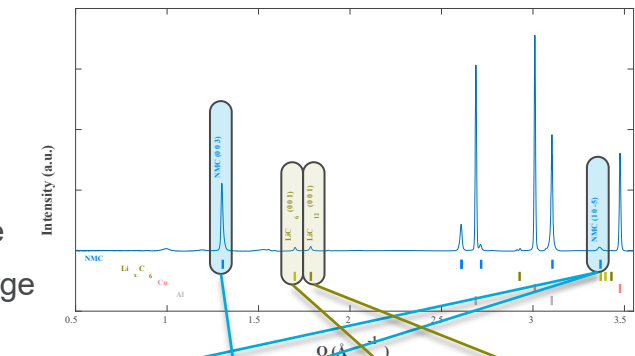
- Single-layer pouch cell
- Round 1 electrodes – ~40 microns thick (1.65 mAh/cm² at C/10)
- 3–4.1 V constant-current/constant-voltage
- 6C-C/2 charge-discharge (10-minute charge cutoff)
- 4 psi stack pressure

Calibration of unit cell volume to lithium content (using NMC half-cell data)

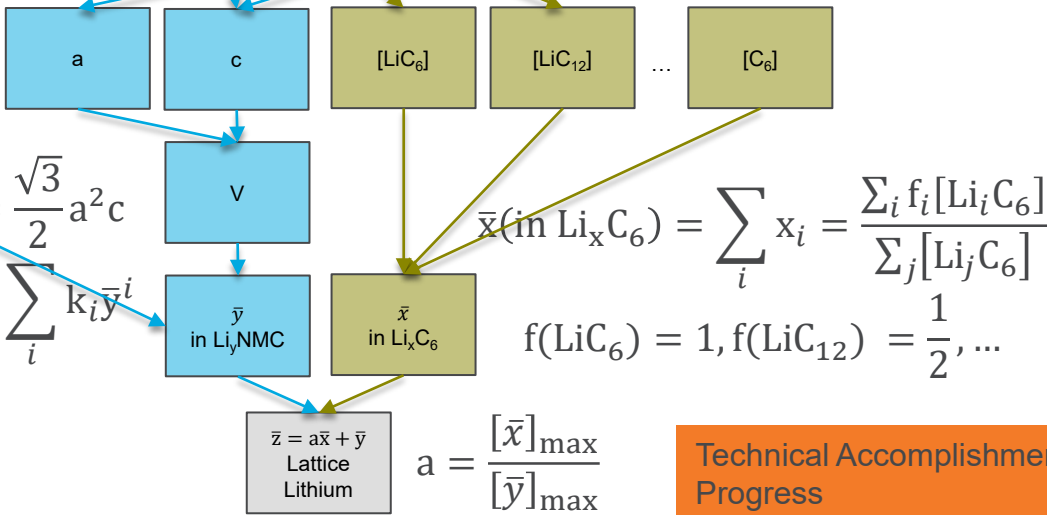


$$V = \frac{\sqrt{3}}{2} a^2 c$$

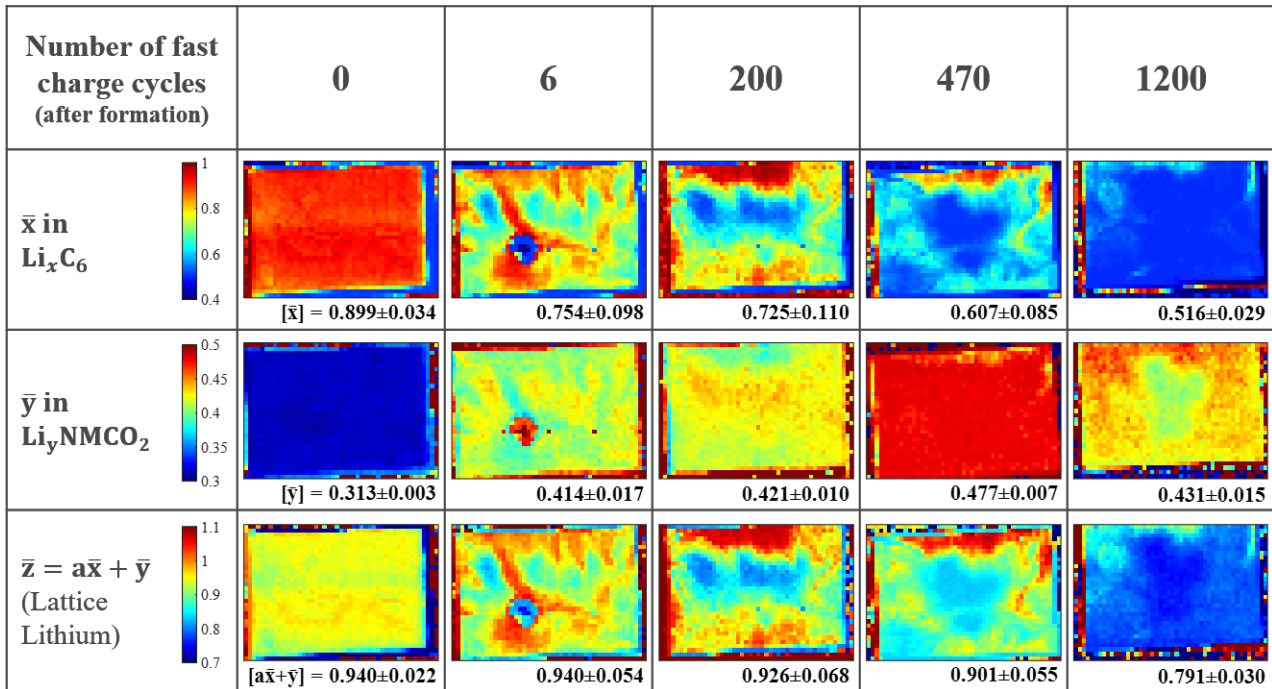
$$V = \sum_i k_i \bar{y}^i$$



Note: Cells preformed with CAMP cycling procedure (tap at 1.5 V, 3x C/10, 3x C/2, 3.5 V safe SOC) under 4 psi pressure on entire cell.

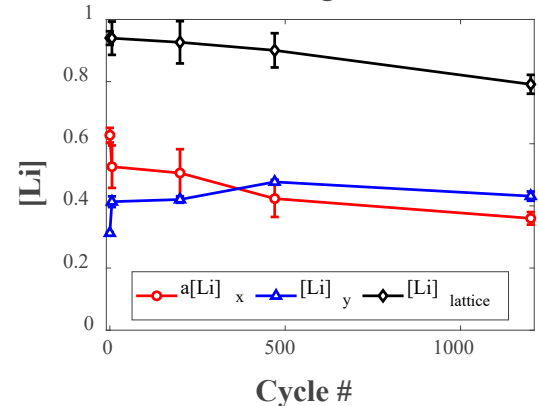


TRACKING LATTICE-LITHIUM HETEROGENEITY AND LITHIUM BALANCE OVER CYCLE LIFE

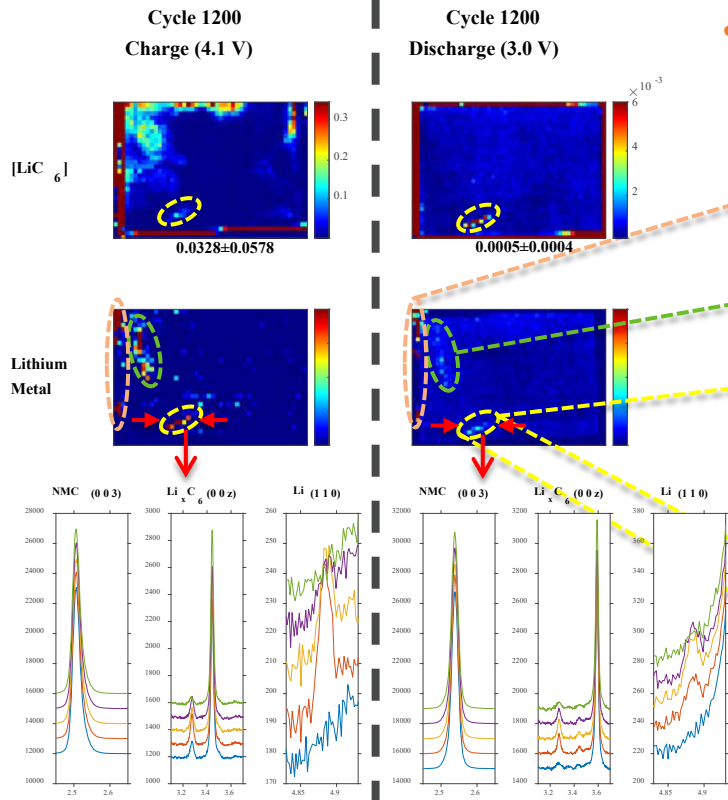


- Fast charging causes heterogeneity

- Initial – outgassing results in low-performance “bubble”
- Intermediate – migration of lithium from center to edge
- End-of-life – Loss of lattice lithium throughout

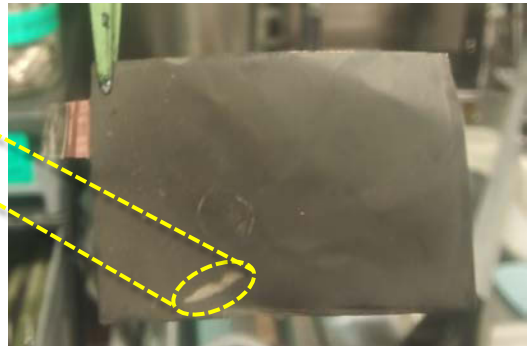


HETEROGENEITY OF LITHIUM PLATING



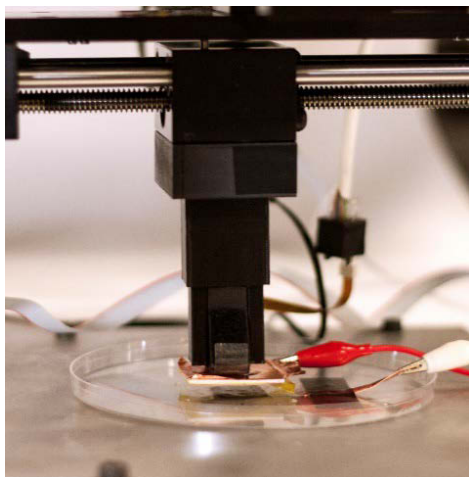
• Lithium plating occurs late in cycle life for R1

- Li plating unrelated to cathode aging effect.
- **Edge** lithium – slightly mismatched electrode prevented “overhang” of excess anode to protect from edge plating, **lithium metal nucleation at edge of cell**.
- Optically invisible lithium “**smudge**” – no corresponding LiC₆, reduced intensity at discharge.
- Optically confirmed lithium “**streak**”
 - Charge – isolated Li (1 1 0) peak, higher LiC₆ concentration than surrounding area without Li plating.
 - Discharge – reduced Li (1 1 0) peak intensity (**Li plating is partially reversible**), corresponding residual **trapped LiC₆**.



Presence of LiC₆ at discharge is marker of Li plating.

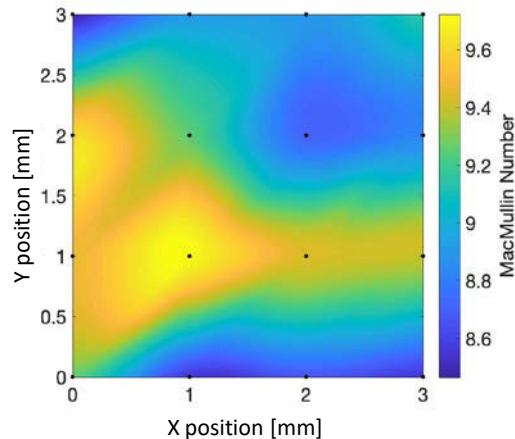
MAPPING OF LOCAL MICROSTRUCTURE PROPERTIES FOR CORRELATING WITH LI PLATING



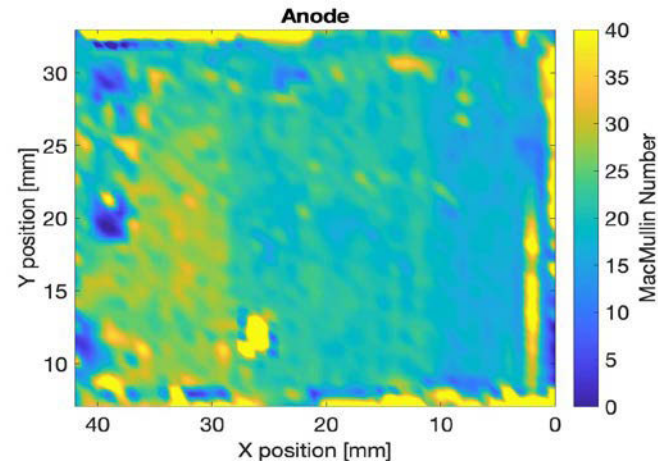
Next Step: Map electrodes prior to cell assembly and compare with XRD mapping

- XYZ stage is used to move a probe across surface of wetted electrode film
- Electrochemical Impedance Spectroscopy measurements are taken at each location and interpreted to create a map of local ionic conductivity
- Electrical resistivity and contact resistance also measured.

Samsung 18650 cell after 250 cycles

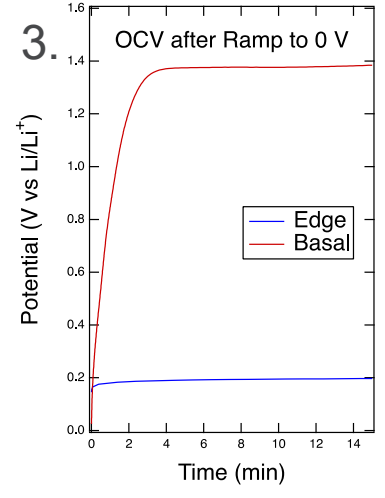
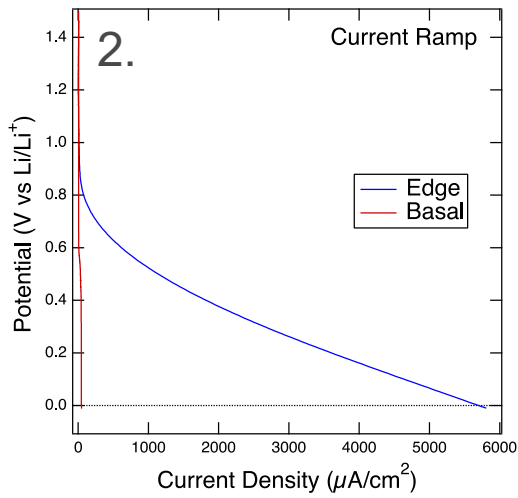
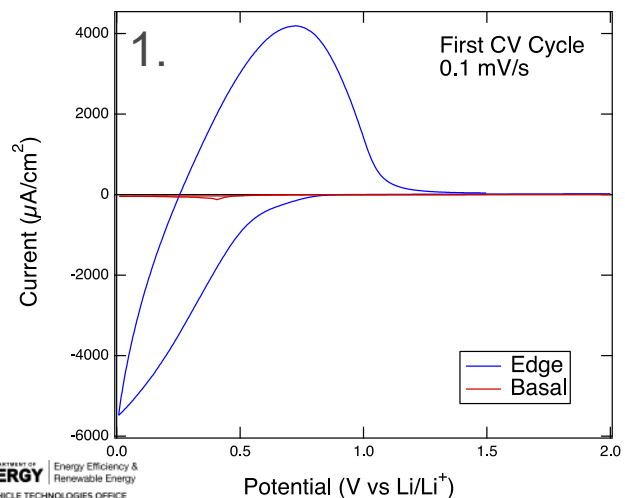
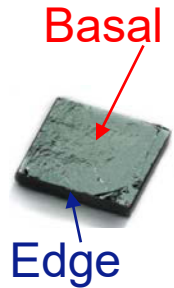


Camp pouch cell after 450 XFC cycles (40 micron thick)



EDGE VS. BASAL GRAPHITE – LITHIATION

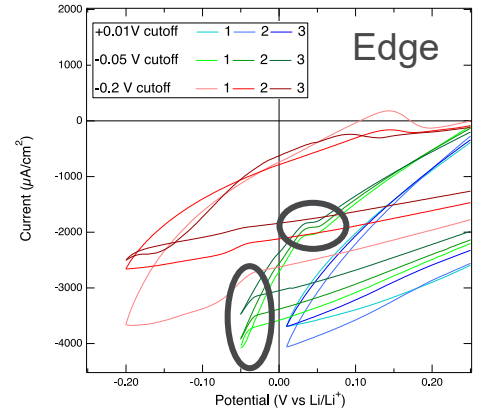
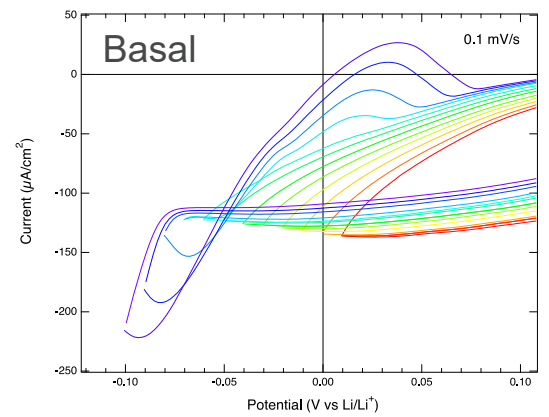
- Electrochemistry on edge and basal plane surfaces of highly oriented pyrolytic graphite yields data on kinetics at graphite surface independent of particle size, binder, or porosity of a composite electrode. Shown below is (1) the first of multiple constant voltage (CV) cycles for formation, (2) a current ramp to -0.01 V, and (3) open-circuit voltage (OCV) relaxation after the ramp.
- Basal plane exhibits low currents, never exceeding $50\text{--}100 \mu\text{A}/\text{cm}^2$ above 0 V. Coulombic efficiency (CE) $< 10\%$ during CV, OCV after ramp relaxes to 1.4 V – no evidence of intercalation, just solvent reduction above 0 V.
- Edge plane exhibits much higher currents and CE $> 95\%$ during CV. Edge planes lithiated reversibly and at up to $6 \text{ mA}/\text{cm}^2$ above 0 V. The same local current density applied to a $3 \text{ mAh}/\text{cm}^2$ composite anode with $\sim 100 \text{ cm}^2_{\text{active}}/\text{cm}^2_{\text{electrode}}$ would correspond to a rate of $\sim 200\text{C}$. The OCV indicates that Li redistributes to form LiC_{24} .



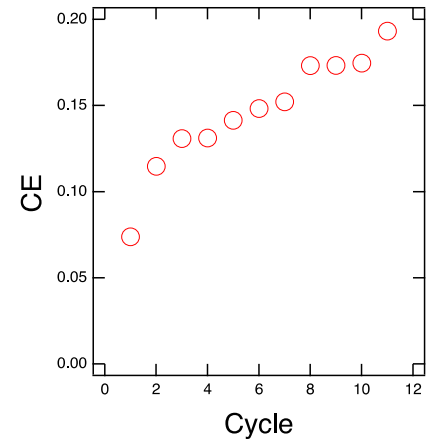
EDGE VS. BASAL PLANE – PLATING

- The lower cutoff voltage of CV on edge and basal planes was varied to detect the plating onset (below).
- Plating occurs on both surfaces, with an onset voltage of -30 mV for edge, -60 mV for basal plane, and with corresponding stripping peaks visible in CV. Once plating on basal planes has nucleated at -60 mV, it can continue at less-negative voltages, depending on current (data not shown).
- CCCV cycling of the basal plane between -0.1 V and $+1.5$ V yielded very low CE (below, right). Li plating on basal surfaces is a very irreversible process and should be avoided.

Edge & Basal, CV with varied cutoff

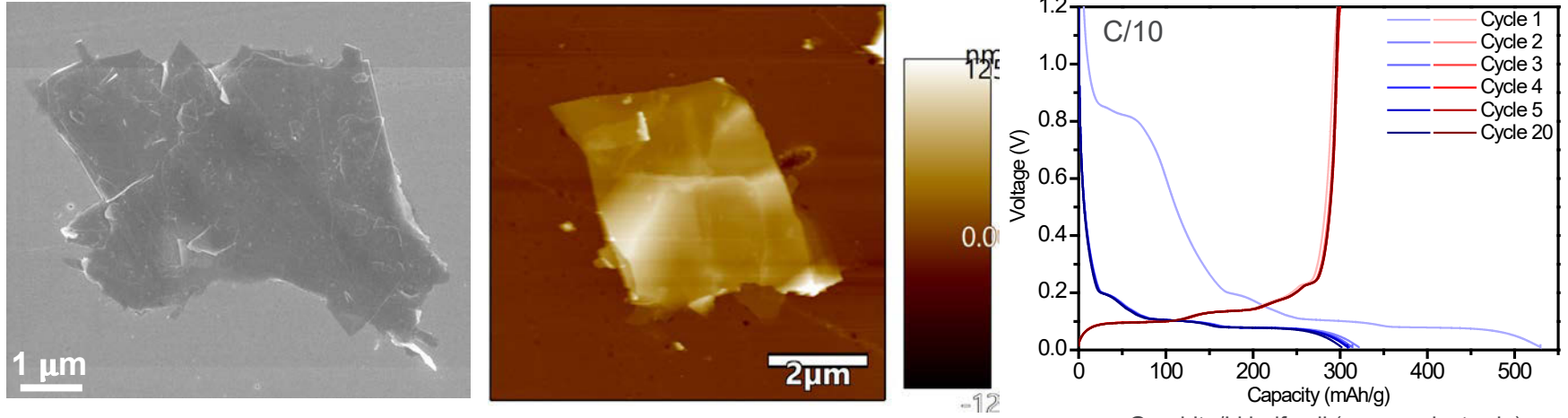


Basal Plating CE



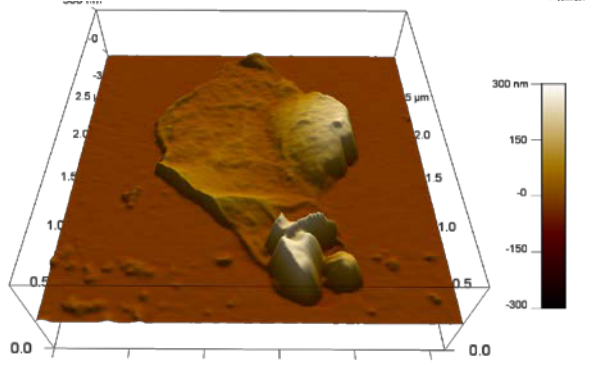
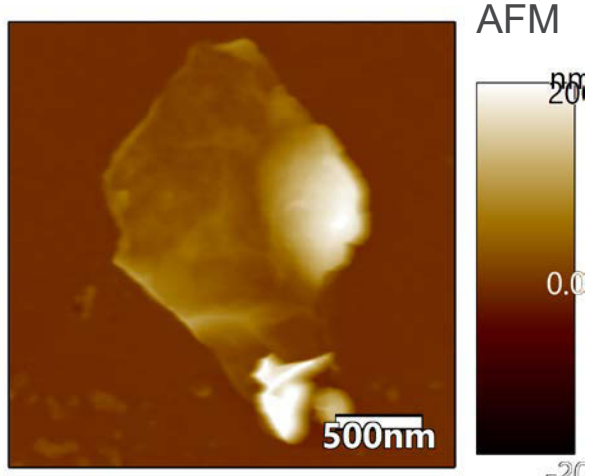
GRAPHITE NANOPATELETS – MODEL SYSTEM FOR STUDYING LI PLATING

- Graphite nanoplatelets: lateral size: 0.5–15 μm ; thickness: 15–100 nm



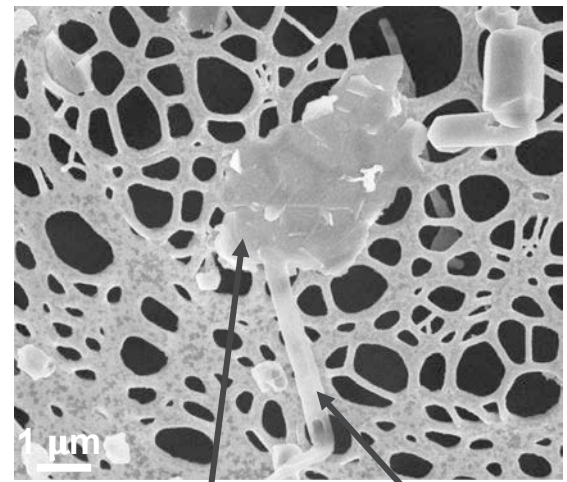
- Small and thin platelets: suitable for atomic force microscope (AFM) studies.
- Distinct basal and edge planes: easy to tell the location of initial Li nucleation.
- Typical (de)lithiation behaviors of graphite: representative model system.

LI PLATING ON GRAPHITE NANOPATELETS

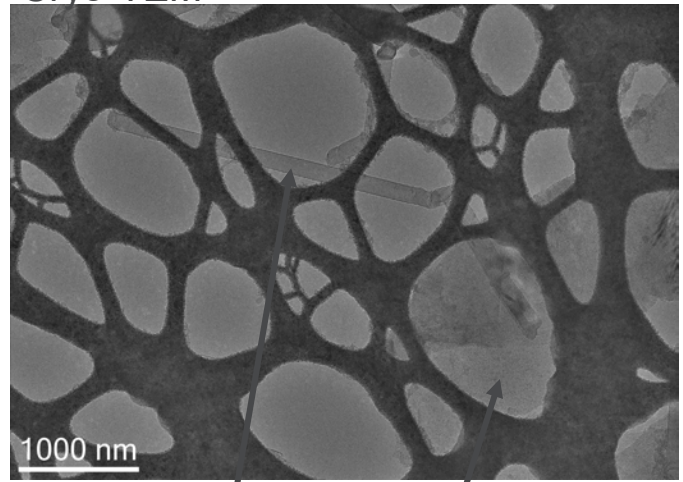


Li plating on graphite nanoplatelets loaded on a transmission electron microscope (TEM) grid

Scanning Electron Microscope



Cryo-TEM

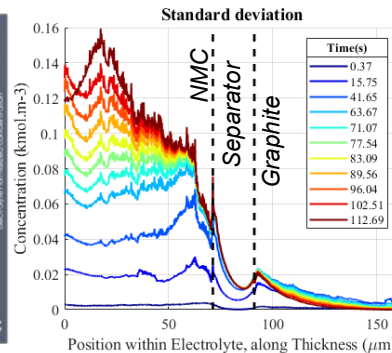
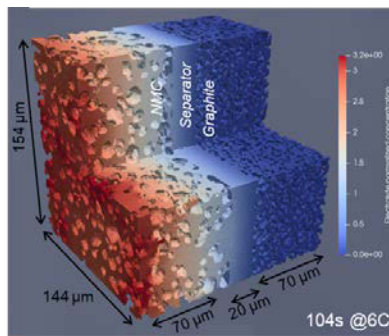


- Successfully plated lithium on individual graphite nanoplatelets.
- Lithium tends to grow at the tip or on the edge planes of graphite.

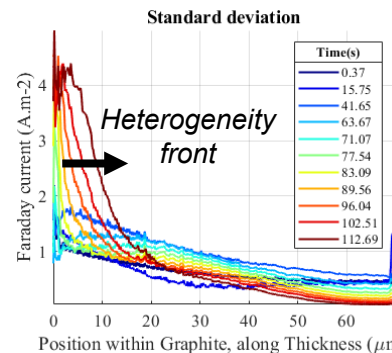
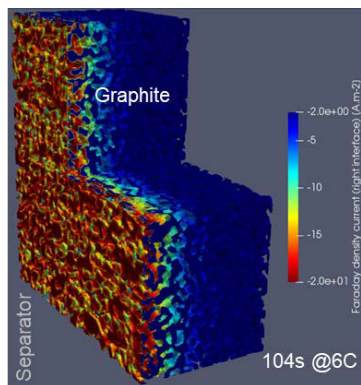
MICROSTRUCTURE-SCALE ELECTROCHEMICAL MODEL EXTENDED TO FULL CELL

Significant in-plane heterogeneities predicted during fast charging

- Micromodel extended to full cell geometry (~30 million degrees of freedom, 300+ processes on NREL high-performance computer [HPC])
- Predicts earlier lithium plating compared with macroscale model (8.5 to 14 s earlier at 6C, 30°C), attributed to microstructure heterogeneity.
 - Plating is not uniform with a 6-mV in-plane difference and 4 s to plate the whole interface once it has started locally
- Significant heterogeneity calculated in the cathode (electrolyte concentration) and in the anode (Faraday current density).



Large heterogeneity (up to 160 mol.m⁻³) localized at the back of the cathode due to high concentration/low diffusion coefficient

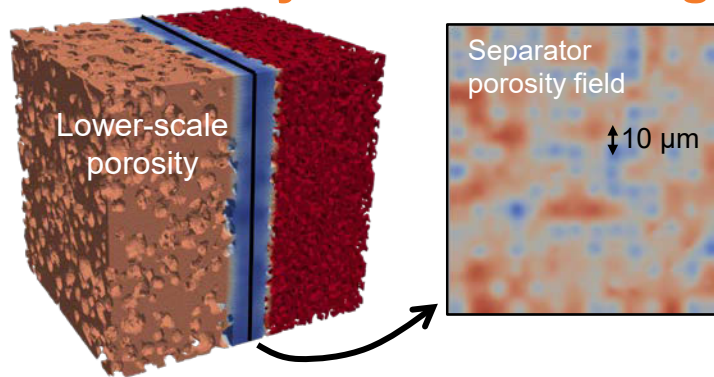


Significant heterogeneity near the anode-separator interface (up to 4 A.m⁻²), that progressively extends deeper in the bulk as graphite locally saturates

LOWER-SCALE HETEROGENEITY AND ADDITIVES

Motivation controlling separator uniformity and decreasing carbon-binder domain (CBD) loading

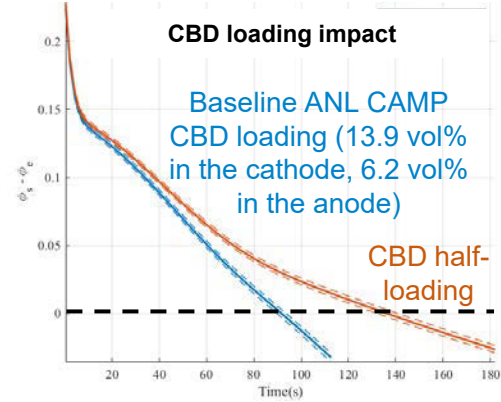
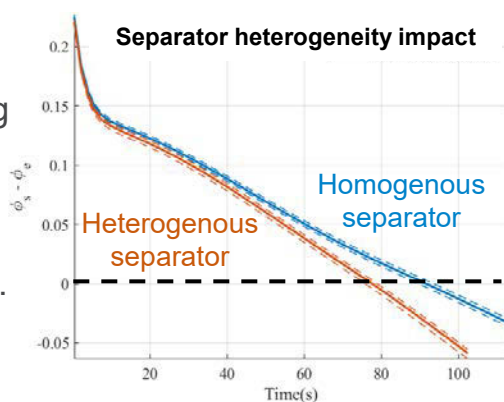
- Separators are porous materials with an intrinsic heterogeneity
 - Separator porosity heterogeneity triggers earlier lithium plating: ± 0.05 porosity with a heterogeneity scale of $10\ \mu\text{m}$ induces an earlier plating of 13 s, 1.5% anode SOC
 - Separator uniformity must be evaluated and maximized
- Carbon binder additives hinder ionic transport in the electrolyte
 - Halving CBD volume loading delays plating from 89 s (18.2% SOC) to 132 s (25.4% SOC) assuming percolation and conductivity are maintained
 - Reducing CBD loading is a promising path.



$$\epsilon_{sep}(x) = \langle \epsilon_{sep} \rangle \pm 0.05$$

with $\langle \epsilon_{sep} \rangle = 0.39$
 Porosity field is randomized in the separator to represent a possible heterogeneity.

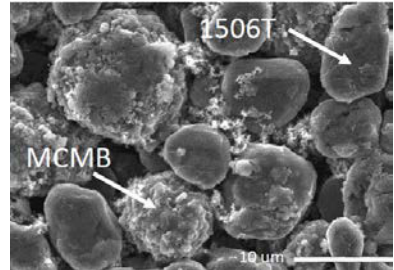
Potential for lithium plating at the separator-anode interface (solid line: mean, dashed lines: extremums)



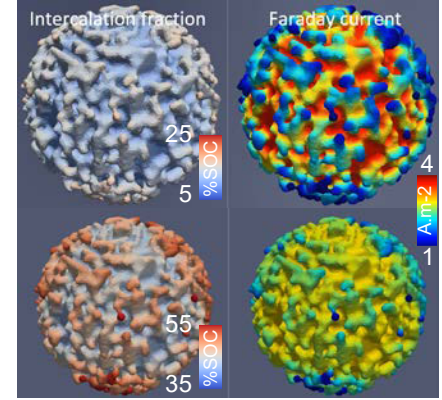
IMPACT OF PARTICLE SURFACE ROUGHNESS

Delaying lithium plating through specific surface area is more effective through particle size, then cracks and surface roughness

- Graphite particles have different surface roughness
 - 1 μm -size surface features induce significant reaction current heterogeneities
 - Heterogeneity varies depending on particle open circuit potential (plateau vs. transition)
- Lithium-plating onset is linearly correlated with specific surface area
 - However, high specific surface is detrimental for calendar life (SEI growth)
 - A unit increment of specific surface area is 20 times more effective in delaying lithium plating at 6C when it results from particle size reduction rather than from surface roughness increase
 - Surface roughness is then to be avoided

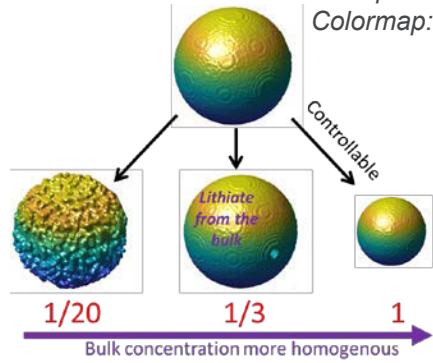


SEM image of two different graphite particles (credits ANL)



At 0.1 SOC, particle uniform at 0.05 SOC
At 0.4 SOC, particle uniform at 0.35 SOC

10 μm -diameter graphite particle lithiated at 6C. Colormap: $\Delta\text{SOC} = 0.2$, $\Delta j = 3 \text{ A.m}^{-2}$, $\langle j \rangle = 2.5 \text{ A.m}^{-2}$



Diameter:

$$\text{SOC}_{\text{plating}} = 1.12 \times Sp + b$$

Cracks:

$$\text{SOC}_{\text{plating}} = 0.351 \times Sp + b'$$

Surface roughness:

$$\text{SOC}_{\text{plating}} = 0.054 \times Sp + b''$$

DEVELOPMENT OF MORE ACCURATE LI-PLATING KINETIC MODEL

- Important to understand the dynamics of lithium deposition and diffusion into the graphite particles for degradation and capacity fade
- Quantify onset and reversibility of plating using coupled Li nucleation model with phase field model for electrodeposition

Stability of nucleus on *electrically charged* substrate is defined by

Gibbs free energy of transformation:

$$\Delta G_t = \left(\Delta G_f + \frac{zF\eta}{\Omega} \right) S_v r^3 + \gamma_{NE} S_A r^2 + (\gamma_{SN} - \gamma_{SE}) \pi r^2 \sin^2 \theta$$

where γ is the interfacial free energy between various components and θ is the contact angle between nucleus and graphite substrate

Critical radius of thermodynamically stable precipitate is given by:

$$r_{eq}^* = - \frac{2\gamma_{NE}\Omega}{zF\eta + \Delta G_f}$$

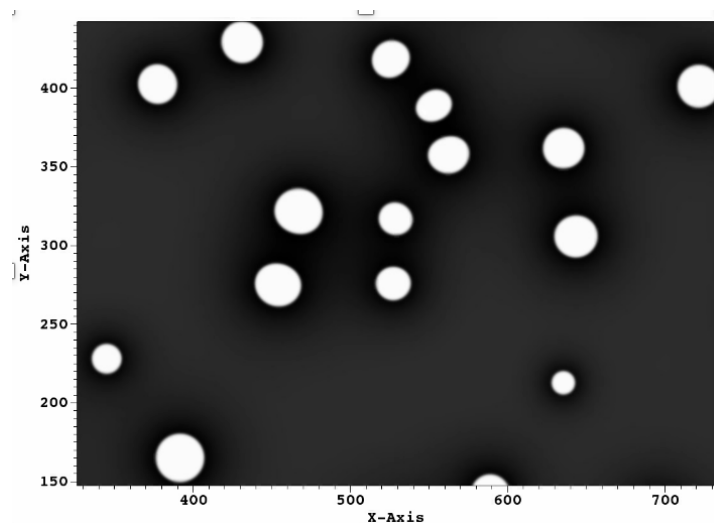
Ely, D.R. et.al., 2013. *Journal of the Electrochemical Society*, 160(4).

COUPLE NUCLEATION MODEL TO ELECTROCHEMICAL/PHASE FIELD MODEL

- Diffuse interface to account for separation of charge (assuming electro-neutrality)
- Explicit introduction of nuclei based on classical nucleation theory
 - Local nucleation probability is calculated based on nucleation rate and local probability.
 - Under nucleation conditions, supercritical nuclei radius is introduced by changing the composition field using smooth gradient interface

Based on classic nucleation theory, the local nucleation rate for critical radii is defined:

$$J^* = ZN\beta \exp\left(\frac{\Delta G^*}{k_B T}\right) \exp\left(\frac{-\tau}{t}\right)$$

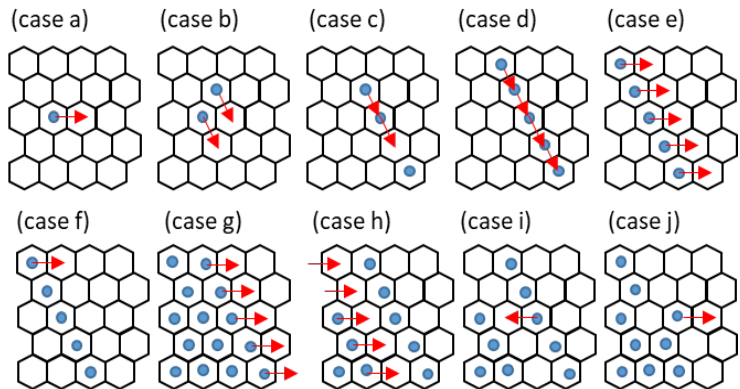


stochastic nucleation simulation of two-phase system

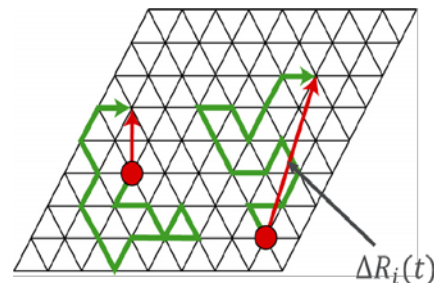
Kinetic Monte Carlo (KMC) Model:

Diffusion coefficient estimation

Configuration	Energy barrier (eV)
Case a: 1 Li-ion (dilute system)	0.34
Case b: 2 Li-ion-cluster perpendicular	0.22
Case c: 2 Li-ion-cluster parallel with vacancy	0.32
Case d: linear cluster parallel displacement	1.10
Case e: linear cluster perpendicular displacement	0.32
Case f: linear cluster perpendicular displacement 1st Li-ion	0.04
Case g: linear cluster moving from high concentration front	0.11
Case h: second linear cluster front moving	0.39
Case i: Li-ion moving back to high concentration front	1.36
Case j: Li-ion second step after moving away from cluster	0.26



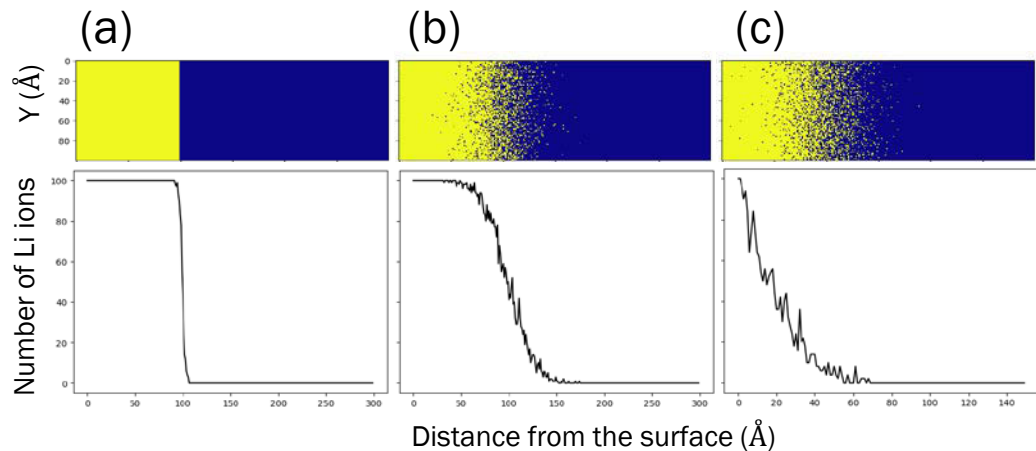
$$D_j = \lim_{t \rightarrow \infty} \left[\frac{1}{4t} \left\langle \frac{1}{N} \left(\sum_{i=1}^N \Delta R_i(t) \right)^2 \right\rangle \right]$$



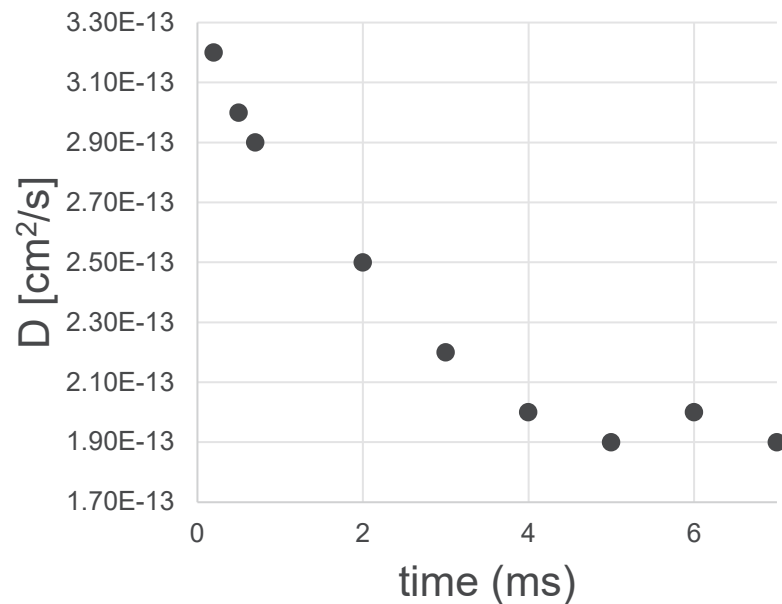
- The KMC model has been implemented to estimate transport properties accounting for changes to hopping energy barrier from local configuration
- Diffusivity has been computed using statistical averages.
- More hopping event cases/configurations will be added.

Kinetic Monte Carlo (KMC) Model:

Diffusion coefficient estimation



Time evolution of Li concentration in the region close to the surface ($x = 0$) of graphite. Li ions (yellow pixels) coordinates diffuse into graphite (blue pixels) with time. Insets represent the content of Li per column. (a) initial state $t = 0$ ms, (b) $t = 3.2$ ms, (c) $t = 6.4$ ms

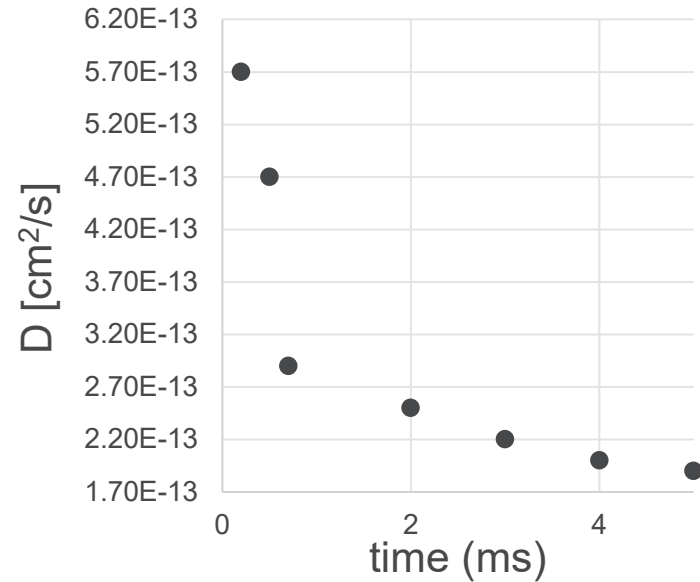
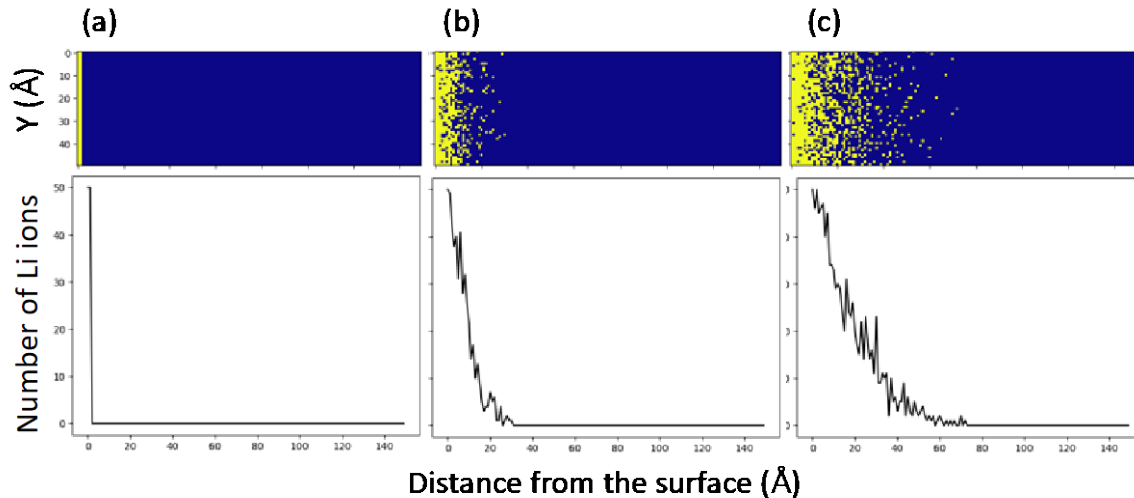


- Initial diffusivity is higher.
- Diffusivity decreases and stabilizes at a lower value.
- Once LiC₆ region is formed, the diffusion is “controlled” by that region (lower diffusivity)
- We still have atomic resolution, which makes the simulation very memory-demanding.

Kinetic Monte Carlo (KMC) model:

Diffusion coefficient estimation

High current rate



- The left boundary is open, and a current rate is set just enough to fill any vacancy at the surface.
- (a) initial state $t = 0$ ms, (b) $t = 0.5$ ms, (c) $t = 5$ ms
- Li at $x = 0$ continually replenished.
- Simulation with a high constant current rate presents an even higher initial diffusivity.
- Diffusivity decreases and stabilizes at a lower value.
- The rapid formation of an LiC_6 region makes the diffusivity constant.
- The time scale for the lower diffusivity regimen seems to be short. We are assessing the effect of the simulation box size and the incorporation of more possible Li hopping events

REMAINING CHALLENGES AND BARRIERS

- Many different heterogeneities at disparate length scales exist simultaneously and isolating the effect of an individual heterogeneity remains challenging
- Improving electrolyte wetting is difficult and may not be improved sufficiently by prolonging formation process
- Challenging to quantify local electrolyte wetting
- Mapping of electrode microstructure properties needs to be performed prior to cell assembly and cycling
 - SOC map and lithium plating pattern may not correlate to any microstructure property
- Determining level/length scale that graphite needs to be modeled to provide insight for XFC
 - Challenging to resolve graphite grain structure within individual particle.

PROPOSED FUTURE WORK*

- Evaluating different strategies to improve electrolyte wetting: rest time, temperature, vacuum pressure, mechanical agitation
- Developing method to quantify local electrolyte wetting via neutron imaging or acoustic measurements
- Overlay maps of SOC, lithium plating, and intercalated lithium with local microstructure properties – determine if correlations exist
- Characterize intercalation and plating process for edge sites with different amounts of lithiation
- Implement detailed lithium-plating kinetics model and experimentally validate
- Inform continuum-scale models with results from KMC atomistic models

*Any proposed future work is subject to change based on funding levels

SUMMARY

- Initial modeling has indicated electrolyte wetting may be the cause of visual lithium-plating patterns
- XRD mapping shows that SOC and cyclable lithium varies substantially across pouch cell after XFC
- Electrochemical microstructure model predicts earlier onset of lithium plating due to heterogeneity compared to traditional Newman/P2D models
- KMC atomistic models predict enhanced diffusion due to local charge accumulation and concerted diffusion
- Sufficient exposed edge sites are required for XFC because exposed basal planes do not have required exchange current density for intercalation
- Lithium tends to nucleate at exposed edge sites or defects.

CONTRIBUTORS AND ACKNOWLEDGEMENTS

Abhi Raj
Alison Dunlop
Alex Quinn
Andy Jansen
Andrew Colclasure
Antony Vamvakeros
Anudeep Mallarapu
Aron Saxon
Bryan McCloskey
Bryant Polzin
Chuntian Cao
Charles Dickerson
Daniel Abraham
Daniel Steingart
Dave Kim
David Brown
David Robertson
David Wragg
Dean Wheeler
Dennis Dees
Donal Finegan
Eongyu Yi
Eric Dufek
Eric McShane
Eva Allen
Francois Usseglio-Viretta
Guoying Chen
Hakim Iddir

Hans-Georg Steinrück
Hansen Wang
Harry Charalambous
Ilya Shkrob
Ira Bloom
James W. Morrisette
Jiayu Wan
Jeffery Allen
Johanna Nelson Weker
Josh Major
John Okasinski
Juan Garcia
Kae Fink
Kandler Smith
Kamila Wiaderek
Kevin Gering
Maha Yusuf
Marca Doeff
Marco DiMichiel
Marco Rodrigues
Matt Keyser
Michael Evans
Michael Toney
Nancy Dietz Rago
Ning Gao
Nitash Balsara
Orkun Fura
Partha Mukherjee

Partha Paul
Parameswara Chinnam
Paul Shearing
Pierre Yao
Quinton Meisner
Ravi Prasher
Robert Kostecki
Ryan Brow
Sang Cheol Kim
Sangwook Kim
Sean Wood
Seoung-Bum Son
Shabbir Ahmed
Sean Lubner
Shriram Santhanagopalan
Srikanth Allu
Steve Trask
Susan Lopykinski
Tanvir Tanim
Uta Ruett
Venkat Srinivasan
Victor Maroni
Vince Battaglia
Vivek Bharadwaj
Vivek Thampy
Volker Schmidt
Wei Tong
Weijie Mai

Wenxiao Huang
William Chueh
William Huang
Xin He
Yang Ren
Yanying Zhu
Yi Cui
Yifen Tsai
Zachary Konz
Zhenzhen Yang



*Support for this work from the Vehicle Technologies Office,
DOE-EERE – Samuel Gillard, Steven Boyd, David Howell*

Thank You

www.nrel.gov

NREL/PR-5400-76710

This work was authored in part by the National Renewable Energy Laboratory, operated by Alliance for Sustainable Energy, LLC, for the U.S. Department of Energy (DOE) under Contract No. DE-AC36-08GO28308. Funding provided by U.S. Department of Energy Office of Energy Efficiency and Renewable Energy Vehicle Technologies Office. The views expressed in the article do not necessarily represent the views of the DOE or the U.S. Government. The U.S. Government retains and the publisher, by accepting the article for publication, acknowledges that the U.S. Government retains a nonexclusive, paid-up, irrevocable, worldwide license to publish or reproduce the published form of this work, or allow others to do so, for U.S. Government purposes.